THE JOURNAL OF PHYSICAL CHEMISTRY B LETTERS

2005, *109,* 21476−21480
Published on Web 10/25/2005

Wave Patterns Driven by Chemomechanical Instabilities in Responsive Gels

Vincent Labrot,[†] Patrick De Kepper,[†] Jacques Boissonade,[†] István Szalai,[†,‡] and Fabienne Gauffre*[,†,§]

Centre de Recherches Paul Pascal (CNRS), Av. Schweitzer, F-33600 Pessac, France, Departement of Inorganic and Analytical Chemistry, L. Eötvös University, P.O. Box 32, H-1518 Budapest 112, Hungary, and Laboratoire des IMRCP, UMR 5623, Université Paul Sabatier, 31062 Toulouse Cedex 09, France

Received: September 9, 2005; In Final Form: October 13, 2005

The first experimental evidence of a chemomechanical mechanism leading to morphogenetic instabilities is demonstrated experimentally. The system consists of a pH-responsive gel that swells at high pH and shrinks at low pH, and a bistable reaction system exhibiting an acid steady state (pH ≈ 2) and an alkaline steady state (pH ≈ 10). Within the gel, the steady state selection depends on the gel size. We show that in a constant and uniform nonequilibrium chemical environment, the responsive gel undergoes large amplitude dynamical deformations under the form of travelling contraction waves and complex spatio-temporal volume oscillations. These deformations are coupled to concentration patterns of protons. We present different sequences of dynamical behaviors observed under various controlled chemical conditions. A simple heuristic model is proposed to account for the observations. These experiments open a new route for pattern formation driven by chemical energy, in soft matter systems.

Introduction

Dissipative processes generally govern self-organization in living systems.[1,2] In reaction−diffusion systems, often used as prototypic systems to study formation and selection of patterns,[1,3,4] the role of the size of the system has been recognized long ago.[1,4] However, still very little is known about the possible morphogenetic instabilities that could result from the interplay of chemical reaction and geometric changes;[5] the so-called "chemomechanical" instabilities. Polyelectrolyte gels are soft and responsive materials that can be used as deformable supports to investigate such instabilities. Indeed, the amount of water uptaken by polyelectrolyte hydrogels critically depends on parameters such as pH, ionic strength, and temperature. Responsive hydrogels have been used to design actuators that convert chemical energy into mechanical operations.[6,7] Also, size oscillations have been obtained by associating a chemically responsive hydrogels with nonlinear oscillating chemical reactions.[8−11] However in all cases, the gel motions are merely slaved to the chemical dynamics, and the responsiveness of the material plays no role in the onset of oscillations. More interestingly, different theoretical studies predict that size or volume changes of a "gel reactor" may play an active role in the development of dynamical instabilities.[12−14] The system presented in this report was specially designed to provide experimental evidence of such chemomechanical instabilities. The two main components of our system are a *N*-isopropylacrylamide-*co*-acrylic acid pH-responsive gel and the acid autocatalytic chlorite/tetrathionate reaction, hereafter called CT.

* Corresponding author. Tel 33.(0)5.61.55.61.43; Fax 33.(0)5.61.55.81.55; E-mail gauffre@chimie.ups-tlse.fr
[†] CNRS.
[‡] L. Eötvös University.
[§] Université Paul Sabatier.

Cross-linked copolymers of *N*-isopropylacrylamide (NIPAAM) and acrylic acid (AA) derivatives are the most common pH-responsive hydrogels.[15−17] For pH values exceeding the pK_a value of the polymer (pK_a ≈ 4), the acid functions grafted on the network deprotonate. Consequently, the free counterions exert an osmotic pressure that causes the network to swell by water uptake. Conversely, at pH below the pK_a, the gel network becomes uncharged and reduces volume by expelling part of the solvent, especially at temperatures equal to or above 35 °C, where the uncharged network becomes grossly hydrophobic.

To interplay with this pH-responsive hydrogel, we selected the CT reaction because it exhibits bistability between two chemical states separated by a large pH difference that encompasses the pK_a of the NIPAMM-*co*-AA hydrogels. Although the detailed kinetics of the CT reaction is still not fully understood,[18] in the range of concentrations used in our experiments, it can be satisfactorily described by simple models[19−21] based on the overall stoichiometric relation

$$7ClO_2^- + 2S_4O_6^{2-} + 6H_2O \rightarrow 7Cl^- + 8SO_4^{2-} + 12H^+$$

associated with an autocatalytic empirical kinetic law,

$$-\frac{d[ClO_2^-]}{dt} = k[ClO_2^-][S_4O_6^{2-}][H^+]^2$$

Such reaction is characterized by an induction time followed by a sudden switch to chemical equilibrium, accompanied by a large drop.

Continuously fed reactors are essential tools to study nonlinear chemical dynamics in sustained conditions. The homogeneous behaviors are studied in continuous stirred tank reactors (CSTR) permanently fed with constant flows of fresh reactants. For

10.1021/jp055095b CCC: $30.25

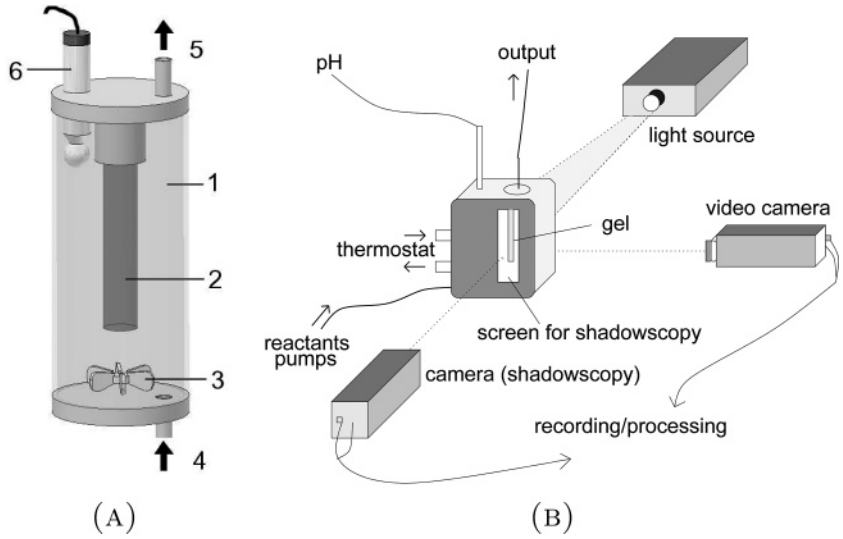

Figure 1. The reactor. (A) Schematic representation of the principles of an open spatial reactor with a cylindrical gel geometry. (1) Continuous stirred tank reactor (CSTR); (2) cylindrical piece of soft hydrogel, hung by one end; (3) fast stirring turbine; (4) inlet flow port for fresh reagents; (5) outlet flow port; (6) pH electrode. Colored chemical patterns or deformations of the gel are monitored by CCD cameras, either through a direct view or shadowscopy. (B) Overview of the experimental setup.

spatial pattern studies, one-side-fed-reactors (OSFRs) are commonly used.[4] They consist of a piece of inert gel diffusively fed from one side by contact with the homogeneous contents of a CSTR.

When autocatalytic reactions are operated in a CSTR, one generally observes bistability between two branches of steady states, corresponding respectively to (i) nearly unreacted compositions and (ii) compositions close to that of the thermodynamical equilibrium.[22] Systems exhibiting bistability in a CSTR can also exhibit spatial bistability in an OSFR.[21,23−25] One state is obtained when recovery through diffusive exchanges occurs on a shorter time scale than the induction time of the reaction, and the other when the reaction is faster than diffusive recovery. In spherical or cylindrical pieces of gel diffusively fed from their environment, the stability of such spatial states naturally depends on the gel radius, since the characteristic penetration times of the chemicals depend on this distance. It is shown theoretically and experimentally that the switch between the two spatial states occurs with hysteresis as a function of such geometric parameters.

When a CSTR is fed with an alkaline solution of reagents of the CT reaction, the unreacted branch (pH ≈10) and the reacted branch (pH ≈2) are simultaneously stable over a large range of parameter values.[21,23] In typical OSFR experiments, the gel is immersed in a solution maintained on the unreacted branch. Then, two different stable concentration profiles can develop between the surface and the core of the gel. In the first case (unreacted), the gel contents are totally alkaline, whereas in the second case (reacted) the solution within the gel is acid, except for a thin alkaline boundary layer located at the interface with the CSTR contents.[21,23]

In some conditions the relatively faster diffusivity of proton, the activator of the reaction, can lead to an oscillatory reaction diffusion instability in an OSFR.[21,23,26,27] In the present experiments, this instability is totally quenched by the weak acid functions polymerized within the gel network.

Materials and Methods

Gel Synthesis. Hydrogels were prepared by free radical copolymerization of acrylic acid and *N*-isopropylacrylamide ([AA]/[NIPAM] = 0.03), using 2,2-azobis(isobutyronitrile) (0.2 mol %) in dioxane (35 wt % monomers, all appropriately purified) as the initiator and *N*,*N*′-methylenebisacrylamide (0.8 mol %) as cross-linker. Gelation was carried out in silicone tubes (internal diameters from 0.5 to 1.7 mm) under nitrogen atmosphere at 75 °C for 24 h. After removal from their molds, the gel cylinders were cut in pieces approximately 3 cm long and washed in methanol/water mixtures (100/0, 75/25, 50/50 and 25/75 vol % for 1 day each), and then in an aqueous chloroform solution (1 vol %, 3 days).

Experimental Setup. The continuous stirred tank reactor (Figure 1) (internal volume = 43 mL) is made of transparent Plexiglas and is optically polished. It is in contact with a thermostated bath set at 35 °C and is equipped with a pH electrode. The cylinder of gel is glued by one end to a stopper introduced at the top of the reactor so that in the course of an experiment it can be removed to apply an acid perturbation. A turbine-like magnetic stirrer creates a hydrodynamic vortex beneath the gel that ensures a strong mixing of the solution. The feeding solutions were stored in four separated reservoirs containing, respectively, an alkaline sodium chlorite solution ($[NaClO_2] = 2 \times 10^{-1}$ M, $[NaOH] = 1.5 \times 10^{-4}$ M), an alkaline potassium tetrathionate solution ($[K_2S_4O_6] = 5 \times 10^{-2}$ M, $[NaOH] = 1.5 \times 10^{-4}$ M), and two sodium hydroxide solutions of different concentrations. The solutions were pumped by precision piston pumps (Pharmacia P500) and premixed just before entering into the reactor at the level of the turbine. The flows of chlorite and tetrathionate solutions were maintained, respectively, at 47 mL/h and 53 mL/h, and the sum of the two sodium hydroxide solutions at 50 mL/h. The ratio between the flows of these two sodium hydroxide solutions were varied to tune the total amount of sodium hydroxide introduced in the reactor. The state of the gel was followed by black and white CCD cameras, either by a direct view through the plexiglass wall of the reactor or by projecting a deflected light image of the gel on a screen (shadowscopy). This technique is most suitable for visualizing the curvatures and the zones with high gradients of refraction index in transparent objects. The light source is a standard slide projector. The cameras are connected to a time lapse VCR and to a frame grabber. Methyl red (pK_a = 5), a color indicator that changes from yellow (basic) to red (acidic), was added to the solutions to directly visualize the

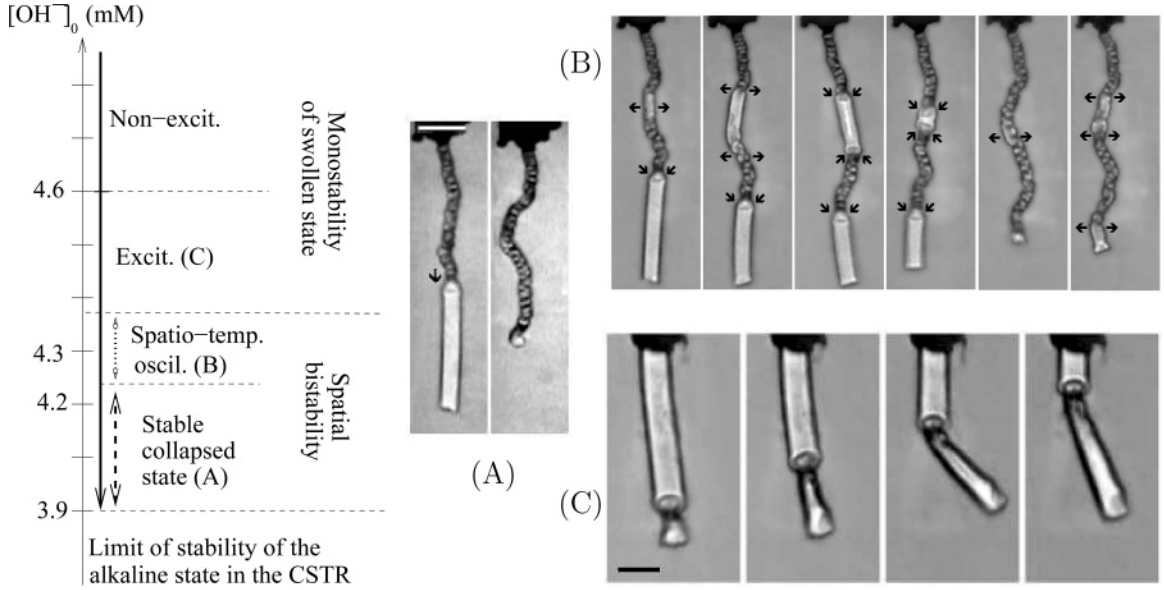

Figure 2. Asymptotic states of the pH-responsive gel. The full, dashed, and dotted vertical arrows respectively delineate the stability domain of the swollen (alkaline), collapsed (acid), and oscillatory states. CSTR conditions: $[ClO_2^-]_0 = 6.32 \times 10^{-2}$ M; $[S_4O_6^{2-}]_0 = 1.8 \times 10^{-2}$ M; residence time = 18.5 min; temperature = 35 °C. All pictures taken by shadowscopy technique. (A) The stable collapsed state (top part) gradually invades the stable swollen state (bottom part). Feed conditions corresponding to the spatial bistability domain:$[OH^-]_0 = 4.2 \times 10^{-3}$ M with a gel of 1.2 mm diameter in the swollen state. (B) Complex spatio-temporal shrinking/swelling oscillations of a cylinder of gel observed at the limit of stability of the collapsed state. Sequence of views taken after an acid perturbation of the swollen state was made at the top of the cylinder. The collapsed state gradually invades the swollen state, but behind the wake of this interface some parts of the cylinder reswell and shrink back. Arrows point the directions of the main local size changes. The intervals of time between snapshots are 18, 14, 11, 50, 26 min; $[OH^-]_0 = 4.3 \times 10^{-3}$ M; other conditions same as A. (C) Large amplitude traveling "bottleneck" obtained after an acid perturbation was made at the tip of a swollen hydrogel cylinder in the "excitable" domain. Wave velocity $\approx$ 5.6 mm/hr. Time interval between snapshots, from left to right: 21, 30, 20 min; Scale = 4 mm. The contraction wave may induce some buckling of the cylinder, due to microscopic inhomogeneities in the polymer network. The corresponding movie in MPEG format is available as Supporting Information.

propagation of acid pulses. The use of this specific indicator makes it possible to observe the acid zones of the gel (in red) across the yellow solution. Before starting an experiment, the gel is maintained in the reactor that is constantly fed with the desired reactant flows for at least 3 h. Then, an acid perturbation can be applied by removing the stopper holding the gel and gently touching the gel at a particular spot with a paper soaked in a 0.02 M H_2SO_4 solution. The gel is then placed back in the CSTR as before.

Results

Our present design of a suspended cylindrical gel immersed in a CSTR allows for unconstrained geometric changes of the responsive material (Figure 1). The cylindrical gels (typical length 30 mm, diameter 1 to 3 mm) are immersed into the reactor fed with fresh alkaline solutions of the CT reactants. The concentration $[OH^-]_0$ of the hydroxyl ions in the mixed feed stream is used as the expandable control parameter because the reaction kinetics strongly depends on its value. The pH within the gel and the gel radius are the observable responses of the system. As mentioned before, when operated in CSTR, the CT reaction exhibits bistability between a branch of alkaline states and a branch of acid states. In the present experiments, the solution in the CSTR is always maintained on the alkaline steady-state branch, i.e., $[OH^-]_0$ is kept over the value $[OH^-]_0^{lim} = 0.77 \times 10^{-3}$ M, beyond which the system switches to the acid branch. In these conditions, whatever the value of $[OH^-]_0$, if the gel is initially alkaline or neutral, it settles in a stable swollen and transparent state. In this case the chemical composition in the gel is very close to that in the CSTR, as it was shown in previous publications.[23] However, when a strong acid perturbation is made at one end of the cylinder, the relaxation dynamics of the perturbation and the asymptotic state depend on the value of $[OH^-]_0$ (Figure 2). The asymptotic states that can be attained after the perturbation are: (i) a transparent swollen state, (ii) a turbid collapsed state (Figure 2A, right), (iii) a complex spatio-temporal oscillatory (volume oscillations) state (Figure 2B). Also, in certain conditions the acid perturbation initiates a transient contraction wave (Figure 2C). In the following we elaborate on the development of these different behaviors observed after an initial acid perturbation.

For values slightly above $[OH^-]_0^{lim}$, after an acid perturbation, the perturbed end of the gel locally switches to the collapsed state. An interface between the collapsed and the swollen states develops and propagates as the collapsed state overtakes the swollen state (Figure 2A, left). The velocity of the interface is of the order of 1 cm/hour and decreases with increasing $[OH^-]_0$. Eventually, the stable, fully shrunken cylinder of gel is obtained (Figure 2A, right). The gel is turbid, crumpled, and kinked at many locations. Its total length measures approximately half of the initial length in the fully swollen state. The complex, long lasting spatio-temporal oscillations between the swollen and shrunken states (Figure 2B) are observed in a narrow domain beyond a critical $[OH^-]_0$ value. Volume changes occur randomly at different locations along the gel cylinder. In the swelling stage, the swelling starts in a small area of the gel and progressively expands radially and laterally at the same time. At some point the swelling process stops and a clear interface forms between the swollen and the collapsed states; eventually this occurs on both sides of the swollen area. Then, both interfaces propagate inwardly inside the swollen state, causing the swollen area to fully return to the collapsed state. This complex spatio-temporal behavior occurs either when, starting from the stable collapsed state, the

Figure 3. Direct close-up view of a traveling pulse in the excitability domain. The image is colorized to emphasize the different regions: gray areas correspond to alkaline compositions (gel and surrounding solution), red area corresponds to acid composition in the gel and yellow marks the turbid part of the acid area. In true colors the acid area is also red due to the acidic form of the dye.

value of $[OH^-]_0$ is increased beyond a critical value or by a local acid perturbation of the swollen state in the same range of parameter. Thus, there is a domain of parameters in which the gel exhibits spatial bistability, between the swollen state and either the fully shrunken state or the state of complex oscillations (Figure 2). Note that when an interface between the swollen and the shrunken states is created, the shrunken state always propagates into the swollen state, whereas a stationary interface or an interface moving in the opposite direction was never observed. Thus in the bistable region, the shrunken state has a larger relative stability than the swollen state.

If the gel has settled in the shrunken or the oscillatory state and the control parameter $[OH^-]_0$ is further increased beyond the bistability domain, the gel swells back and turns clear. However, if a new local acid perturbation is then applied to this swollen cylinder, a transient contracted zone, associated with a turbidity area, forms and propagates undamped into the unperturbed swollen part of the cylinder (Figure 2C). The contraction wave takes a stable bottleneck shape with a local diameter drop reaching up to 50% that of the swollen part. This traveling polymer density wave exhibits all the dynamic characteristics of an excitability wave.[29] Using methyl red as a pH color indicator, one observes that this contraction wave is associated with an acid wave (Figure 3). The acid wave exhibits a "drop" shape, which is in agreement with the shape of the acid−alkaline interface previously observed with annular gel reactors[21,27] or conical gels.[26,28] However, the associated turbid contraction wave exhibits a hollow "ring" shape. This is due to the fact that the collapse first occurs in the acid−alkaline boundary area where the pH gradient is very strong. This result was previously observed in numerical studies.[13] As for the interface in Figure 2A, the velocity of the wave decreases with increasing $[OH^-]_0$.

Eventually, at higher values of $[OH^-]_0$, the alkaline swollen state loses this excitability property.

Discussion and Model

We propose the following empirical chemomechanical model to account for the experimental observations. The model is based on the bistability property of the chemical solution within the gel associated to the feedback induced by the change of the gel radius, as sketched in the (size; core pH) diagram presented Figure 4. Consider a disk shape slice of our cylindrical gel in the swollen alkaline state immersed in the CSTR with an $[OH^-]_0$ value in the spatial bistable domain (0). When a supercritical acid perturbation is applied to the disk (1), the chemical state of the gel contents rapidly switches to the acid core state (2), inducing a shrinkage of the radius of the disk. The radius size eventually crosses the stability limit of the branch of acid core

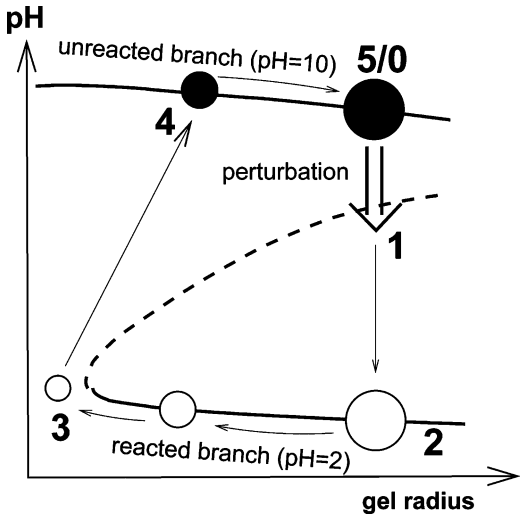

Figure 4. Heuristic model for a chemomechanical excitability mechanism in the case of a disk of gel. The trajectory of the system is plotted in the (gel radius, pH in the gel core) phase plane. Solid and dotted lines represent, respectively, stable and unstable states; white and black disks represent, respectively, the alkaline (unreacted) and acid (reacted) states within the gel.

state (3). This in turn makes the contents of the gel gradually turn back to the fully alkaline state (4). Consequently, the gel swells back to its initial stable radius as the solvent and reactants diffuse back in (5). Such a switching and slow drift mechanism mimics a standard excitable system.[29] Consider now, that the above slice is in contact with the rest of the cylinder in the swollen alkaline state. The local acid core state can contaminate by diffusion the neighboring alkaline region and makes it also cross the excitability threshold. An acid front forms and propagates in the swollen part of the gel. At the back of this acid front a shrinkage of the radius is expected, and the radius reaches a minimum (point (3) in Figure 4). Because the chemical composition and the swelling now exclusively depend on the diffusive exchanges from the surface, the recovery process is slow, consistent with the experimental observations (Figure 2C). Numerical calculations on a similar chemomechanical mechanism were shown to lead to the self-oscillation of a chemoresponsive bead of gel when the size changes of the piece of gel are large enough to cross both upper and lower size limits of the spatial bistability domain.[12,13]

Figure 5 schematically represents the domain of spatial bistability and of the monostable alkaline state for CT in an OSFR.[21,23] Perturbations can be applied at different locations on the dashed line representing the initial radius of the gel in the swollen alkaline state (r_b). If such a perturbation is applied in the monostable alkaline area of the diagram (NE in Figure 5), then no change occurs because the gel is non excitable. Volume changes of the gel after an acid perturbation in the bistable domain induce a vertical displacement of the system in the diagram, as represented by the arrows. Contraction waves (Figure 2C) are obtained when the collapse is large enough for the system to cross the boundary limit (arrow C), provoking the transition to the alkaline state followed by the reswelling of the gel (arrow C′). A transition to the stable collapsed state (Figure 2A) is observed when the gel radius remains within the bistable domain (arrow A). As a consequence, the contraction of the gel shifts the effective bistability domain to higher radii (dashed line in Figure 5) as compared to its stability in a nonresponsive gel (full line in Figure 5). In a restricted parameter region just below the new stability limit of the acid core state, the alkaline state acquires chemomechanical excitability proper-

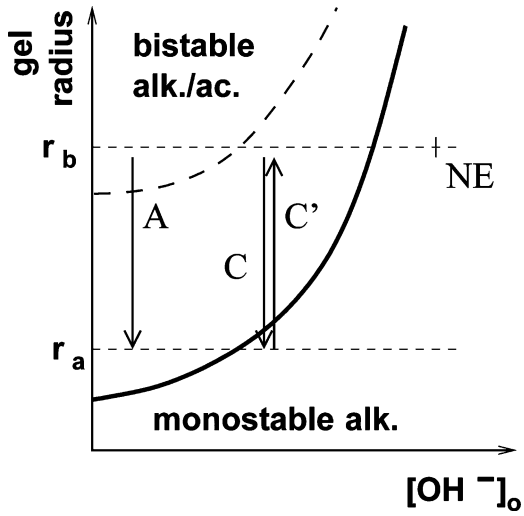

Figure 5. Schematic representation of the spatial bistability limit between the fully alkaline state and the acid core state in the plane ($[OH^-]_0$, gel radius). The limit of stability of the alkaline state in the CSTR is taken as the origin of the $[OH^-]_0$ axis. Full line curve corresponds to the stability limit of the acid core state for a nonresponsive gel. Dash curve corresponds to the "new" stability limit of the acid core state in a responsive gel. The size r_a and r_b represent respectively the radius of the same gel in the acidic (collapsed) and alkaline (swollen) state. In the monostable alkaline state the swollen gel is non excitable (NE). Arrow (A) represents the transition toward the stable collapsed state after a supercritical acid perturbation of the swollen state, corresponding to Figure 2A. Arrows (C) and (C′) represent the trajectory in the radii changes that leads to the excitable behavior illustrated in the snapshots of Figure 2C.

ties. The large amplitude spatio-temporal swelling/shrinking oscillations (Figure 2B), which are observed in a narrow range of parameters, are probably due to the presence of size inhomogeneities close to the critical stability of the acid core state (dashed line in Figure 5). Indeed, in the collapsed state the gel cylinders exhibit a crumpled surface. The radius of the cylinders thus significantly varies along the axis, so that at some thin zones the acid state may loose stability, the gel becomes alkaline, swells, and reenters the former bistability domain, while other neighboring parts would remain in the acid state. Extended contacts between the alkaline re-swollen parts and the acid collapsed parts may trigger a new acid front[26] in these swollen areas that then shrink again. The cycle repeats more or less periodically with some randomness on the location.

Conclusion

This report demonstrates that associating the spatial bistability of an acid autocatalytic reaction and a pH-responsive gel can produce dynamical deformations in the gel. Depending on the reactant feed conditions, the volume of the gel can exhibit bistability (swollen/shrunken), but also traveling contraction waves and complex oscillations. Such dynamical behavior occurs because the volume changes of the pH-responsive gel can destabilize one of the stationary states of the pH-bistable reaction and make the other exhibit excitability properties. In contrast with other systems in which the gel deformation is slaved to the chemical dynamics, deformations of large amplitude (several mm) have been produced with this mechanism. We envisage that such a mechanism can also produce stationnary morphological patterns, but until now we have been unsuccessful in this direction. This is the first experimental demonstration that in soft responsive material systems geometry or size can feed back into a chemical process to generate a new class of chemomechanical dissipative structures.

Acknowledgment. This work was supported by CNRS and Région Aquitaine. We thank E. Dulos for fruitful discussions.

Supporting Information Available: A video clip (MPEG format) corresponding to the snapshots in Figure 2C (excitable behavior) is available free of charge via the Internet at http://pubs.acs.org.

References and Notes

(1) Murray, J. D. Mathematical Biology II: Spatial Models and Biomedical Applications in *Interdiciplinary Applied Mathematics*; Springer: New York, 2003; Vol. 18.
(2) Maini, P. K.; Murray, J. D.; Tranquillo, R. T. *Phys. Rep.* **1988**, *171*, 59−84.
(3) Turing, A. M. *Philos. Trans. R. Soc. London Ser. B* **1952**, *237*, 37.
(4) Kapral, R.; Showalter, K. *Chemical Patterns and Waves*; Klüwer: Amsterdam, 1995.
(5) Cummings, F. W. *Physica D* **1994**, *79*, 146−163.
(6) Osada, Y.; Ross-Murphy, *Sci. Am.* **1993**, *268*, 82−87.
(7) Kaneko, D.; Gong, J.-P.; Osada, Y. *J. Mater. Chem.* **2002**, *12*, 2169−2177.
(8) Yoshida, R.; Takahashi, T.; Yamaguchi T.; Ichijo, H. *J. Am. Chem. Soc.* **1996**, *118*, 5134−5135.
(9) Yoshida, R.; Kokufuta, E.; Yamaguchi, T. *Chaos* **1999**, *9*, 260−266.
(10) Yoshida, R.; Tanaka, M.; Onodera, S.; Yamaguchi, T.; Kokufuta, E. *J. Phys. Chem. A* **2000**, *104*, 7549−7555.
(11) Crook, C. J.; Smith, A.; Jones, R. A. L.; Ryan, A. J. *Phys. Chem. Chem. Phys.* **2002**, *4*, 1367−1369.
(12) Boissonade, J. *Phys. Rev. Lett.* **2003**, *90*, 188302.
(13) Boissonade, J. *Chaos* **2005**, *15*, 023703.
(14) Borckmans, P.; Benyaich, K.; De Wit, A.; Dewel, G. In *Nonlinear Dynamics in Polymeric Systems*; Pojman J. A., Tran-Cong-Miyata, Q., Eds.; ACS Symposium Series 869; American Chemical Society: Washington, DC, 2003; pp 58−70.
(15) Cussler, E. L.; Stokar, M. R.; Varberg, J. E. *AIChE J.* **1984**, *30*, 578−582.
(16) Huglin, M.; Liu, Y.; Velada, J. *Polymer* **1997**, *38*, 5785−5791.
(17) Lee, Y. M.; Yoo, M. K.; Sung, Y. K.; Cho, C. S. *Polymer* **2000**, *41*, 5713−5719.
(18) Horváth, A.; Nagypál, I.; Peintler, G.; Epstein, I. R. *J. Am. Chem. Soc.* **2004**, *126*, 6246−6247.
(19) Nagypál, I.; Epstein, I. R. *J. Phys. Chem.* **1986**, *90*, 6285−6292.
(20) Horváth, D.; Tóth, Á. *J. Chem. Phys.* **1998**, *108*, 1447−1451.
(21) Fuentes, M.; Kuperman, M. N.; Boissonade, J.; Dulos, E.; Gauffre, F.; De Kepper, P. *Phys. Rev. E* **2002**, *66* (056205).
(22) Epstein, I.; Pojman, J. *An Introduction to Nonlinear Chemical Dynamics*; Oxford University Press: New York, 1998.
(23) Boissonade, J.; Dulos, E.; Gauffre, F.; Kuperman, M. N.; De Kepper, P. *Faraday Discuss.* **2001**, *120*, 353−361.
(24) Blanchedeau, P.; Boissonade, J.; De Kepper, P. *Physica D* **2000**, *147* 283−299.
(25) Blanchedeau, P.; Boissonade, J. *Phys. Rev. Lett.* **1998**, *81*, 5007−5010.
(26) Gauffre, F.; Labrot, V.; Boissonade, J.; De Kepper, P.; Dulos, E. *J. Phys. Chem. A* **2003**, *107*, 4452−4456.
(27) Szalai, I.; Gauffre, F.; Labrot, V.; Boissonade, J.; De Kepper, P. *J. Phys. Chem. A* **2005**, *109*, 7843−7849.
(28) Strier, D., E.; Boissonade, J. *Phys. Rev. E* **2004**, *70*, 016210.
(29) Mikhailov, A. *Foundations of Synergetics I. Distributed Active Systems*, Springer: Berlin, 1994.